Journal of Alloys and Compounds 708 (2017) 1245–1249

Contents lists available at ScienceDirect

Journal of Alloys and Compounds

journal homepage: http://www.elsevier.com/locate/jalcom

Magnetic properties of large-scaled MnBi bulk magnets

Sumin Kim [a], Hongjae Moon [a], Hwaebong Jung [a], Su-Min Kim [b], Hyun-Sook Lee [a, **], Haein Choi-Yim [b], Wooyoung Lee [a, *]

[a] Department of Materials Science and Engineering, Yonsei University, 262 Seongsanno, Seodaemun-gu, Seoul 120-749, Republic of Korea
[b] Department of Physics, Sookmyung Women's University, Seoul 140-742, Republic of Korea

ARTICLE INFO

Article history:
Received 19 December 2016
Received in revised form
4 March 2017
Accepted 6 March 2017
Available online 7 March 2017

Keywords:
MnBi bulk
Rapid-solidification
Sintering
Magnetic properties

ABSTRACT

We investigated the magnetic properties of large, compacted, sintered MnBi bulk magnets with dimensions of 20.3 × 15.3 × 10.3 mm^3. To obtain a high content of the low-temperature-phase (LTP) of MnBi in the precursor powders, a new process was implemented and produced about 98 wt% of LTP. To improve the coercive field of MnBi, particle sizes were controlled using different milling techniques. The dependence of magnetic properties of the bulk magnets on the particle size was analyzed. The highest maximum energy product, $(BH)_{max}$, obtained among our samples was 7.3 MGOe. This is the first report of demonstrating high performance in large-sized MnBi bulk magnets.

1. Introduction

The low-temperature-phase (LTP) of MnBi has attracted much attention as a desirable material for high-temperature (~200 °C) applications because of its high uniaxial magnetic anisotropy at room temperature and unusual positive temperature coefficient of coercivity [1–8]. For practical applications of MnBi, there remains the main challenge of fabrication of high-performance bulk magnets with a high maximum energy product $(BH)_{max}$. The formation of pure LTP-MnBi with high volume fraction is difficult because the difference in melting temperature between Mn (1246 °C) and Bi (271 °C) is too large and a peritectic reaction occurs over wide temperature and composition ranges [9]. The unreacted Mn and Bi always appear as minor phases along with the MnBi phase as the result of an incomplete peritectic reaction [10]. Furthermore, the preparation of sintered MnBi bulk magnets with a high level of LTP is still a very challenging task. Mn tends to segregate from MnBi liquid through the peritectic reaction at 446 °C [6], and a partial melting of LTP-MnBi takes place at 262 °C by eutectic reaction as a result of the reaction with Bi to form the Bi-Mn liquid phase [9]. Therefore, various synthesis techniques have been employed to achieve high-quality MnBi powder. While most results have been reported for MnBi powders and melt-spun ribbons, not much work has been done on the fabrication of MnBi sintered magnets.

One of the important process steps in the fabrication of a bulk magnet is the preparation of a suitable precursor powder. The melt-spin rapid-solidification method has been able to consistently produce over 95 wt% pure LTP [2,5–7,11,12]. Recent results obtained with the conventional method of arc-melting followed by grinding and thermal annealing also yielded over 90 wt% single phase [8,9,13–16]. In particular, Xie et al. recently reported an LTP content in MnBi powder of up to 96 wt% (from the calculation, the ratio of the M_S of MnBi to the theoretical M_S value) achieved using low-energy ball-milling at room temperature [16]. The highest LTP content in MnBi powder of up to 97 wt% has been achieved using low-energy ball-milling at low temperature (−120 °C), this is attributed to suspension of excessive decomposition of MnBi that occurs during ordinary room-temperature ball-milling [13]. In addition, magnetic separation has been suggested as a method to enhance the initial LTP content (e.g. from 60 wt% to 90 wt% [15]). Although highly pure MnBi powder can possibly be produced, the fabrication of sintered MnBi bulk magnets of high quality is still very limited. This is because the decomposition of LTP occurs at a relatively low temperature, as mentioned above, and the degradation of magnetic properties of a bulk magnet compared to that of powder is consequentially inevitable during the sintering process. In practice, the values of $(BH)_{max}$ reached in the powder (9 MGOe

* Corresponding author.
** Corresponding author.
E-mail addresses: h-slee@yonsei.ac.kr (H.-S. Lee), wooyoung@yonsei.ac.kr (W. Lee).

http://dx.doi.org/10.1016/j.jallcom.2017.03.067
0925-8388/

[14] and 11.9 MGOe [9]) showed a significant decrease in the bulk (5.8 MGOe [14] and 7.8 MGOe [9]). The highest value of $(BH)_{max}$ of MnBi bulk magnets reported so far is 8.4 MGOe [17], but this is far below the theoretical limit of 17.6 MGOe [18]. In particular, the reported values of $(BH)_{max}$ of bulk magnets were obtained from only a part of an original bulk sample using a vibrating sample magnetometer (VSM) or a superconducting quantum interference device magnetometer (SQUID) [3,9,13,14,17,19]. The magnetic properties of bulk magnets are strongly dependent on the details of the synthesis process and should be measured from large-scaled samples. In this work, a *BH* loop tracer, which is a general tool for measuring magnetic properties of hard bulk magnets, was employed to characterize the magnetic properties of the large-scaled MnBi bulk magnets. Further improvement of $(BH)_{max}$ can be accomplished by optimizing the balance between remnant magnetization (M_r) and coercivity (H_c). For this optimization, high content of LTP-MnBi in the initial powder and full densification and good alignment of its grains in the final bulk are required. An appropriate combination of powder synthesis method and consolidation technique still needs to be found. In this paper, we report on the magnetic properties of MnBi bulk magnets with large dimension compared to others previously reported.

2. Experiment

MnBi powders were prepared by the following procedure: melt-spinning, cold-pressing, annealing, magnetic separation, and grinding. Commercial raw materials of Mn (99.99%) and Bi (99.99%) were mixed in the desired atomic ratios. To obtain higher LTP content, excess Mn was added into $Mn_{50}Bi_{50}$, and the optimal amount was adjusted in the variation of x wt% (x = 0, 5, and 7). Ribbons of MnBi were obtained by ejecting the alloy melt from a quartz tube onto the surface of a rotating copper wheel under an argon atmosphere at 50 kPa. To enhance the quenching rate, the tangential speed of the wheel was set at about 55 m/s, and the nozzle diameter of the quartz tube was about 0.25 mm. The melt-spun ribbon was coarsely ground using mortar and pestle. The crushed ribbon was then compressed with an applied pressure of 40 MPa at room temperature to form a cylinder 5 mm in height and 10 mm in diameter. The cylinders were annealed at 300 °C for 20 h in vacuum and coarsely ground. The magnetic separation technique was used to separate the LTP from the non-magnetic phases, such as unreacted Mn and Bi or Mn- and Bi-rich phases, before mechanical grinding. To prepare powders with various particle sizes, conventional ball-milling and jet-milling methods were utilized. Low energy ball milling was performed for different milling times (1.0, 2.0, and 2.5 h) using a planetary mill with a rotation speed of 150 rpm. Jet milling was carried out with an inlet pressure of about 0.34 MPa under N_2 atmosphere. The as-milled powders were compacted to dimensions of 20.3 mm × 15.3 mm × 10.3 mm under an applied pressure of 650 MPa in the presence of a 2 T magnetic field in argon atmosphere at room temperature. The obtained green compact was sintered at 280 °C for 10–20 min with an applied pressure of 350 MPa under vacuum. All sample handling was done in an argon-filled glove box whenever needed (LABstar, MBraun, $p(O_2) < 1$ ppm).

Differential scanning calorimetry (DSC, Perkin-Elmer) was used to study the structural transformation of the non-quenched ingot and quenched melt-spun ribbon under flowing nitrogen gas. The phases grown in the as-spun ribbons and annealed ribbons were characterized by X-ray diffraction (XRD, Bruker D8 Advance with LynxEye) with Cu Kα radiation. The morphology and composition of sintered bulk magnets were investigated using a scanning electron microscope (SEM, JEOL, JSM-7001F) equipped with an energy dispersive X-ray spectroscopy (EDX) system. Microstructures were observed by transmission electron microscopy (TEM, JEOL, JEM-ARM 200F). The particle size distributions of the as-milled MnBi powders prepared with different milling techniques were analyzed using a particle size analyzer (HELOS). Magnetic properties of the hot-compacted MnBi bulk magnets with dimensions of 20.3 × 15.3 × 10.3 mm^3 were measured at room temperature using a hysteresis loop tracer (Robograph RE).

3. Results and discussion

Thermal analyses of the MnBi samples in the form of the as-cast ingot and as-spun ribbons were carried out to investigate the rapid quenching effect on the formation of LTP and to determine an appropriate annealing temperature for high purity LTP. The as-cast ingot and as-spun ribbons were prepared using arc-melting and melt-spinning, respectively, from the raw materials. The differential scanning calorimetry (DSC) scans taken at a heating rate of 40 K/min under flowing N_2 gas are shown in Fig. 1. The DSC curves show that the overall thermal behaviors for the two samples are significantly different. Structural change with increasing temperature, which is indicated by rather sharp endothermic peaks, is clearly observed only in the quenched sample. The three endothermic peaks located at the temperatures of ~265 °C, ~360 °C, and ~465 °C are seen in both samples with different intensities. The three peaks indicate, respectively, melting of Bi-rich eutectic and Bi(Mn) phases, a transformation of LTP to high-temperature phase (HTP), and decomposition of MnBi [6,12,20–23]. With an increasing temperature, the as-cast ingot shows crystallization of some fraction of Bi, Mn_3Bi, and ferromagnetic MnBi, which is signified with a broad exothermic peak at ~150 °C [6,12,20–23], but the quenched ribbon does not. A notable feature is that the LTP formation indicated by the exothermic peak at ~271 °C [6,12,20–23] appears only in the quenched melt-spun ribbon.

Fig. 2(a) shows the X-ray diffraction (XRD) pattern of melt-spun MnBi ribbon synthesized without the ingot-making process. In typical fabrication processes, a rapidly solidified MnBi ribbon is fabricated during the quenching procedure of melt-spinning starting with an ingot previously synthesized by arc-melting. Consequently, volatilization of Mn occurs twice: once in the arc-melt and again in the melt-spin processes. To avoid this, we produced melt-spun MnBi ribbons without arc-melting, thus

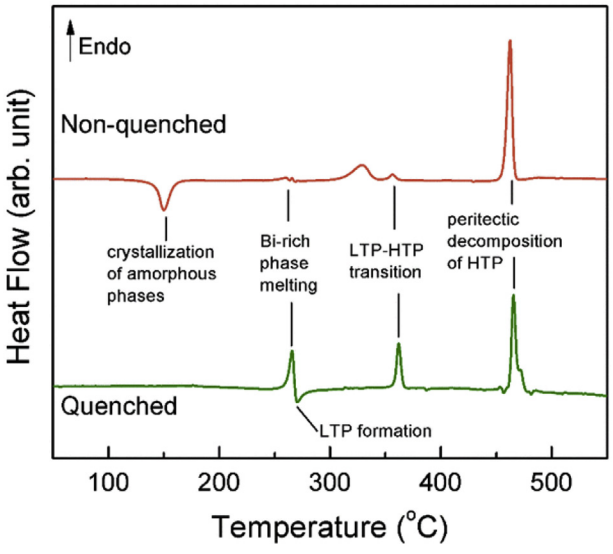

Fig. 1. DSC curves for an as-cast MnBi ingot and an as-spun MnBi ribbon.

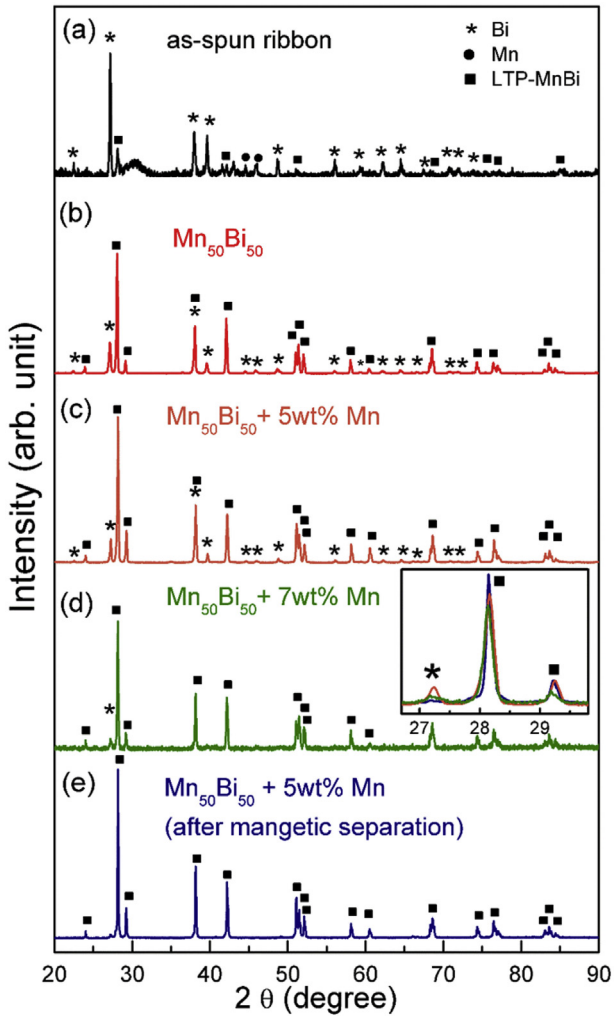

Fig. 2. XRD patterns of (a) the as-spun ribbon without ingot-making process, (b)–(d) the annealed ribbons of $Mn_{50}Bi_{50}$ + *x* Mn (x = 0, 5, and 7 wt%) in the form of compressed cylinders annealed at 300 °C for 20 h after melt-spinning, and (e) the annealed ribbons of $Mn_{50}Bi_{50}$ + 5 wt% Mn after magnetic separation. Inset presents a magnified view of the figures of (b), (c), and (d) near the 2-theta range of the main phase.

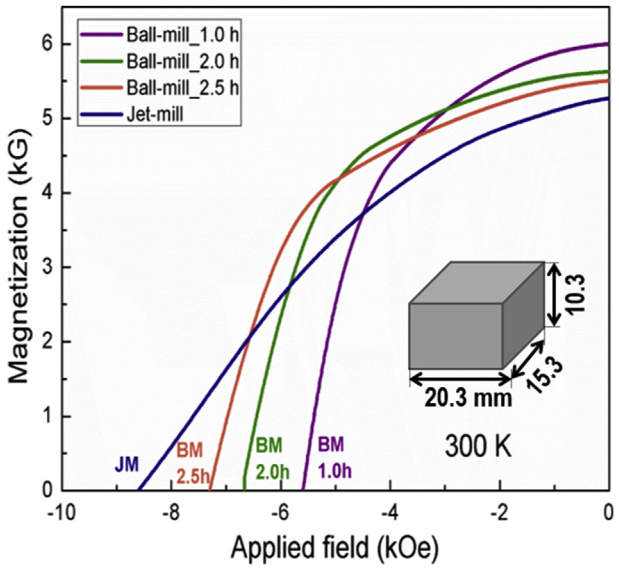

Fig. 3. Demagnetization curves of the final MnBi bulk magnets.

preventing more Mn loss. As shown in Fig. 2(a), a small fraction of LTP-MnBi is already formed even at the melt-spinning process. However, a large amount of unreacted Bi remains, while there is little Mn left. This means that Mn excess is required to get higher LTP content. To balance the composition of Mn and Bi, excess Mn was added to $Mn_{50}Bi_{50}$ in the amount of *x* wt% (*x* = 0, 5, and 7). Before annealing, the melt-spun ribbon was coarsely crushed and compressed into a cylinder at room temperature. The compacted ribbon was annealed for 20 h at 300 °C — a temperature determined from the DSC analysis in Fig. 1. In this procedure, abundant formation of LTP-MnBi is expected because the close contact between ribbons allows Mn, as it readily diffuses, to combine with Bi.

The phases formed in the annealed ribbons of $Mn_{50}Bi_{50}$ + *x*Mn (x = 0, 5, and 7 wt%), which are presented in Fig. 2(b)–(d), indicate that LTP-MnBi is well grown after annealing at 300 °C. As Fig. 2(b) shows, unreacted Bi still appears at $Mn_{50}Bi_{50}$ (*x* = 0) without other phases, but the amount decreases with increasing *x*. At *x* = 7, the unreacted Bi has disappeared, but the peak intensity for LTP has decreased as can be seen in the inset of Fig. 2(d). These results indicate that a high content of well-structured LTP was synthesized at *x* = 5 (Fig. 2(c)). From a refinement analysis, lattice parameters are determined as *a* = 4.2739 Å and *c* = 6.1087 Å, and the weight fraction of pure LTP is about 95.1 wt%. The magnetic LTP fragments are collected from the annealed ribbons of $Mn_{50}Bi_{50}$ +5 wt% Mn by performing magnetic separation. According to the XRD data of the magnetically separated powder (Fig. 2(e)), only LTP-MnBi is present, and the content is increased to 98.1 wt%, which is the highest value obtained from precursor powders so far [5–7,11].

The magnetically-separated fragments of annealed $Mn_{55}Bi_{50}$ ribbons were milled to particles of various sizes by utilizing low-energy ball-milling (BM) and jet-milling (JM) techniques. It has been reported that a remarkable enhancement in coercivity of $Mn_{50}Bi_{50}$ powders has been observed after BM when the milling time is over 1.0 h [7]. Thus, milling times of 1.0 h, 2.0 h, and 2.5 h were used. The as-milled powders were compacted and sintered. The densities of the hot-compacted magnets were in the range of 8.10–8.41 g/cm^3, which corresponds to about 90.0–93.5% of the theoretical density of the MnBi compound (8.99 g/cm^3 [17,24]). The magnetic properties of all samples MnBi bulk magnets with dimensions of 20.3 × 15.3 × 10.3 mm^3 were examined. Fig. 3 shows the demagnetization curves for the MnBi bulk magnets measured under an applied field parallel to the alignment direction at room temperature. The values of magnetic properties (M_r, H_c, and $(BH)_{max}$) obtained from the demagnetization curves in Fig. 3 are presented in Table 1. The MnBi bulk magnets fabricated with BM powders (so-called BM magnets) show that H_c increases and M_r decreases, as the ball-milling time increases. The MnBi bulk magnet fabricated with JM powders (so-called JM magnet) shows more enhanced H_c and more reduced M_r than that in the BM magnets.

The coercivity of sintered magnets like Ba-ferrite ($BaFe_{12}O_{19}$) [25], Sm-Co ($SmCo_5$) [26], or Nd-Fe-B ($Nd_2Fe_{14}B$) [27–30] is

Table 1
Magnetic properties of hot-compacted MnBi bulk magnets.

	H_c [kOe]	M_r [kG]	$(BH)_{max}$ [MGOe]
Ball-mill			
1.0 h	5.6	6.00	7.3
2.0 h	6.7	5.63	6.9
2.5 h	7.3	5.50	6.5
Jet-mill	8.6	5.27	6.1

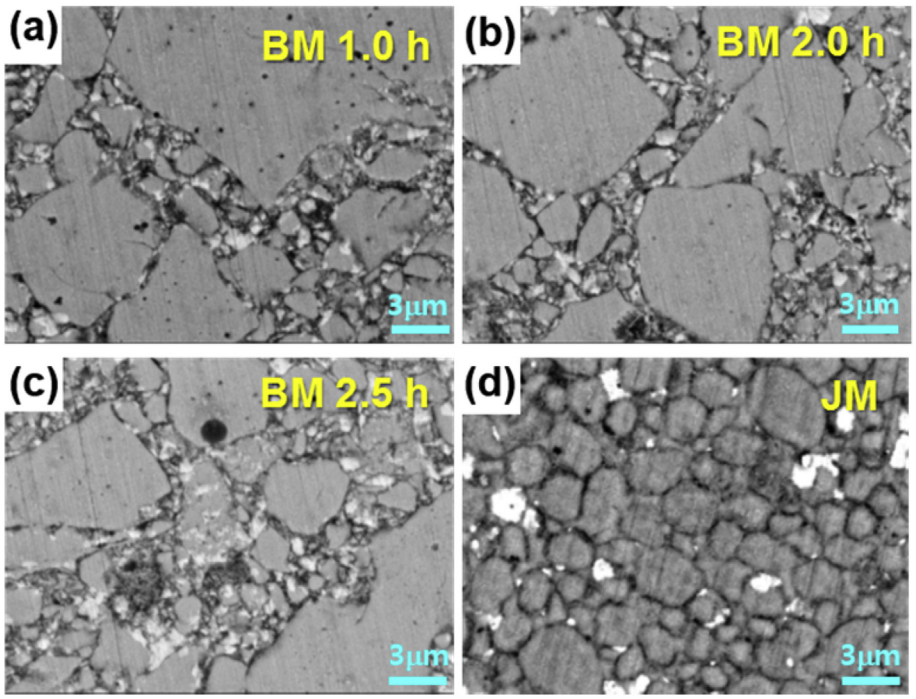

Fig. 4. Back-scatter SEM images of the hot-compacted MnBi bulk magnets prepared with ball-milled (BM) powders with different milling times ((a) 1.0 h, (b) 2.0 h, and (c) 2.5 h) and (d) jet-milled (JM) powders.

affected by the grain size: it has been reported to increase when the mean grain size decreases [25–30]. Therefore, we attempted to investigate the effect of grain size on the coercivity in variously prepared MnBi sintered magnets. The grains in the hot-compacted magnets are shown in the SEM images, recorded with back-scattered electrons, in Fig. 4. An inhomogeneous grain-size distribution is observed in the BM magnets: both small grains (<3 μm) and large grains (>10 μm) (Fig. 4(a)–(c)) are observed. On the other hand, a homogeneous distribution is observed in the JM magnet (Fig. 4(d)). The grain size of sintered magnets varies almost linearly with variations in the mean particle size of the milled powders [27,30]. Therefore, we investigated the magnetic properties of MnBi bulk magnets as a function of the average particle size instead of the average grain size. The average particle sizes are defined as the median diameter at the 50% point of the cumulative distribution, which was obtained using a particle size analyzer. The resultant values are 5.76, 5.23, and 4.62 μm for BM powders for 1.0, 2.0, and 2.5 h, respectively, and 3.01 μm for the JM powder. The average particle size decreased with increasing milling time and the JM technique gives rise to much smaller particles.

H_c and M_r are plotted in Fig. 5(a) as a function of average particle sizes. As the particle size is reduced, H_c increases and M_r decreases. The increase in H_c can be explained by the particle size effect observed in hard magnets [25–30]. The obtained H_c is in the range of 5.6–8.6 kOe, which is similar to values reported by other groups (5.0–7.9 kOe) [8,11,13,14,17]. The decrease in M_r can be explained by the reduction in the volume fraction of ferromagnetic LTP-MnBi due to stress causing decomposition during the milling process [10,16] and due to thermal decomposition during the compaction process [9,14]. Microstructural and compositional analyses of a hot-compacted MnBi magnet, which was fabricated with powders milled for 2.0 h, were performed using TEM and EDX (see Fig. 6). Three phases, namely, LTP-MnBi, Bi-rich, and Mn-rich phases, were observed, indicating that phase segregation occurred due to thermal decomposition during the hot compaction process [9,14]. These results support the hypothesis that MnBi decomposition causes the reduction in M_r, which occurs due to the reduced volume fraction of the magnetic phase of LTP. The lowest M_r in the JM magnet means that a jet-mill process gives rise to the greater phase segregation of the LTP.

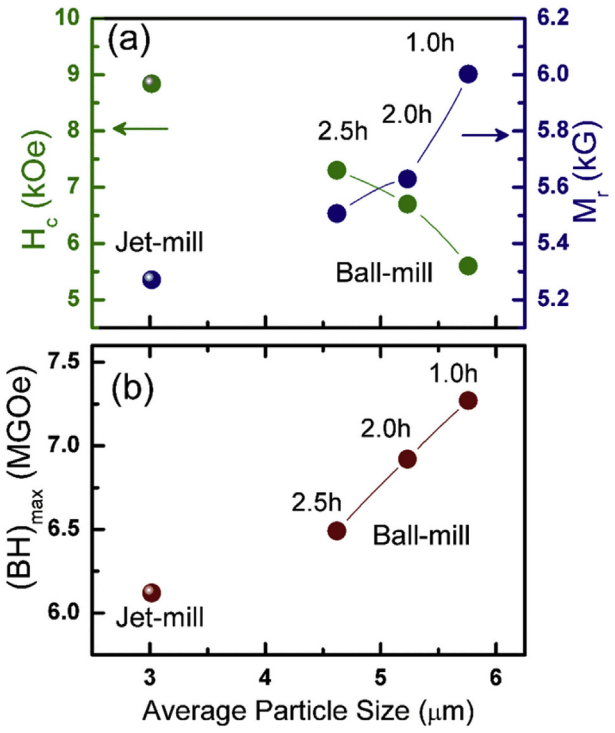

Fig. 5. (a) H_c and M_r, (b) $(BH)_{max}$ of the MnBi bulk magnets as a function of average particle size.

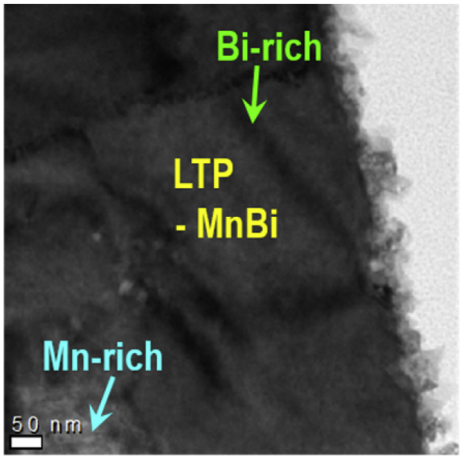

Fig. 6. TEM images of the hot-compacted MnBi magnet fabricated using powder as-milled for 2.0 h.

The values of $(BH)_{max}$ for the MnBi bulk magnets are shown in Fig. 5(b) and Table 1. The highest value for the 1.0 h BM magnet was 7.3 MGOe, which is higher than the values of $(BH)_{max}$ for 2.0 h and 2.5 h BM and JM. It is noted that this is the first report on such large-scaled MnBi bulk magnets. However, further improvement of $(BH)_{max}$ to reach the theoretical value is still needed for practical applications. Further investigation is required on powder refinement and hot compaction to reduce LTP decomposition and magnetic pressing to attain good alignment of grains.

4. Conclusions

We investigated the magnetic properties of MnBi bulk magnets with large scale. We have tried a new procedure for the preparation of high-quality precursor powder to attain high LTP content: melt-spinning, cold-pressing, annealing, magnetic separation, and grinding. By adopting the new process, the amount of LTP obtained was ~98 wt%, which is the highest value compared to that presented in the literature for precursor powders. The improvement of coercivity was accomplished by controlling the particle size using different milling techniques. The magnetic properties of the hot-compacted MnBi bulk magnets were investigated using the entire as-prepared bulk sample without cutting. The highest value of $(BH)_{max}$ obtained for the largest bulk magnets ever made was 7.3 MGOe. Our results show that our process can yield high-performance in MnBi bulk magnets with larger dimensions.

Acknowledgements

This work was supported by the Priority Research Centers Program (2009-0093823) through the National Research Foundation of Korea (NRF). H-S Lee thanks to the Basic Science Research Program through the National Research Foundation of Korea (NRF) funded by the Ministry of Science, ICT & Future Planning (2016-11-1280).

References

[1] T. Chen, W.E. Stutius, The phase transformation and physical properties of the MnBi and $Mn_{1.08}Bi$ compounds, IEEE Trans. Magn. 10 (1974) 581–586.
[2] X. Guo, X. Chen, Z. Altounian, J.O. Stromolsen, Magnetic-properties of MnBi prepared by rapid solidification, Phys. Rev. B 46 (1992) 14578–14582.
[3] N.V. Rama Rao, A.M. Gabay, W.F. Li, G.C. Hadjipanayis, Nanostructured bulk MnBi magnets fabricated by hot compaction of cryomilled powders, J. Phys. D. Appl. Phys. 46 (2013) 265001.
[4] J.B. Yang, K. Kamaraju, W.B. Yelon, W.J. James, Q. Cai, A. Bollero, Magnetic properties of the MnBi intermetallic compound, Appl. Phys. Lett. 79 (2001) 1846–1848.
[5] J.B. Yang, Y.B. Yang, X.G. Chen, X.B. Ma, J.Z. Han, Y.C. Yang, S. Guo, A.R. Yan, Q.Z. Huang, M.M. Wu, D.F. Chen, Anisotropic nanocrystalline MnBi with high coercivity at high temperature, Appl. Phys. Lett. 99 (2011) 082505.
[6] Y.B. Yang, X.G. Chen, S. Guo, A.R. Yan, Q.Z. Huang, M.M. Wu, D.F. Chen, Y.C. Yang, J.B. Yang, Temperature dependences of structure and coercivity for melt-spun MnBi compound, J. Magn. Magn. Mater 330 (2013) 106–110.
[7] Y.B. Yang, X.G. Chen, R. Wu, J.Z. Wei, X.B. Ma, J.Z. Han, H.L. Du, S.Q. Liu, C.S. Wang, Y.C. Yang, Y. Zhang, J.B. Yang, Preparation and magnetic properties of MnBi, J. Appl. Phys. 111 (2012) 07E312.
[8] D.T. Zhang, S. Cao, M. Yue, W.Q. Liu, J.X. Zhang, Y. Qiang, Structural and magnetic properties of bulk MnBi permanent magnets, J. Appl. Phys. 109 (2011) 07A722.
[9] J. Cui, J.P. Choi, G. Li, E. Polikarpov, J. Darsell, N. Overman, M. Olszta, D. Schreiber, M. Bowden, T. Droubay, M.J. Kramer, N.A. Zarkevich, L.L. Wang, D.D. Johnson, M. Marinescu, I. Takeuchi, Q.Z. Huang, H. Wu, H. Reeve, N.V. Vuong, J.P. Liu, Thermal stability of MnBi magnetic materials, J. Phys. Condens. Matter 26 (2014) 064212.
[10] N.V. Rama Rao, G.C. Hadjipanayis, Influence of jet milling process parameters on particle size, phase formation and magnetic properties of MnBi alloy, J. Alloy. Compd. 629 (2015) 80–83.
[11] K.W. Moon, K.W. Jeon, M. Kang, M.K. Kang, Y. Byun, J.B. Kim, H. Kim, J. Kim, Synthesis and magnetic properties of MnBi(LTP) magnets with high-energy product, IEEE Trans. Magn. 50 (2014) 2103804.
[12] X. Guo, A. Zaluska, Z. Altounian, J.O. Stromolsen, The formation of single-phase equiatomic MnBi by rapid solidification, J. Mater. Res. 5 (1990) 2646–2651.
[13] V.V. Nguyen, N. Poudyal, X.B. Liu, J.P. Liu, K. Sun, M.J. Kramer, J. Cui, Novel processing of high-performance MnBi magnets, Mater. Res. Express 1 (2014) 036108.
[14] N.V. Rama Rao, A.M. Gabay, G.C. Hadjipanayis, Anisotropic fully dense MnBi permanent magnet with high energy product and high coercivity at elevated temperatures, J. Phys. D. Appl. Phys. 46 (2013) 062001.
[15] J.B. Yang, W.B. Yelon, W.J. James, Q. Cai, M. Kornecki, S. Roy, N. Ali, P. l'Heritier, Crystal structure, magnetic properties and electronic structure of the MnBi intermetallic compound, J. Phys. Condens. Matter 14 (2002) 6509–6519.
[16] W. Xie, E. Polikarpov, J.P. Choi, M.E. Bowden, K.W. Sun, J. Cui, Effect of ball milling and heat treatment process on MnBi powders magnetic properties, J. Alloy. Compd. 680 (2016) 1–5.
[17] N. Poudyal, X.B. Liu, W. Wang, V. Vuong Nguyen, Y. Ma, K. Gandha, K. Elkins, J. Ping Liu, K. Sun, M.J. Kramer, J. Cui, Processing of MnBi bulk magnets with enhanced energy product, AIP Adv. 6 (2016) 056004.
[18] J. Park, Y.K. Hong, J.J. Lee, W.C. Lee, S.G. Kim, C.J. Choi, Electronic structure and maximum energy product of MnBi, Metals 4 (2014) 455–464.
[19] Y.C. Chen, G. Gregori, A. Leineweber, F. Qu, C.C. Chen, T. Tietze, H. Kronmuller, G. Schutz, E. Goering, Unique high-temperature performance of highly condensed MnBi permanent magnets, Scr. Mater 107 (2015) 131–135.
[20] C.S. Lakshmi, R.W. Smith, Effect of rapid quenching on the magnetic and structural-properties of Bi-MnBi composites, J. Mater. Sci. 25 (1990) 465–471.
[21] X. Guo, Z. Altounian, J.O. Stromolsen, Formation of MnBi ferromagnetic phases through crystallization of the amorphous phase, J. Appl. Phys. 69 (1991) 6067–6069.
[22] F.X. Yin, N.J. Gu, T. Shigematsu, N. Nakanishi, Sintering formation of low temperature phase MnBi and its disordering in mechanical milling, J. Appl. Phys. 91 (2002) 8525–8527.
[23] S. Saha, R.T. Obermyer, B.J. Zande, V.K. Chandhok, S. Simizu, S.G. Sankar, J.A. Horton, Magnetic properties of the low-temperature phase of MnBi, J. Appl. Phys. 91 (2002) 8525–8527.
[24] K. Isogai, M. Matsuura, N. Tezuka, S. Sugimoto, Magnetic properties of MnBi fine particles fabricated using hydrogen plasma metal reaction, Mater. Trans. 54 (2013) 1673–1677.
[25] H. Stäblein, Hard ferrites and plastoferrites, in: E.P. Wohlfarth (Ed.), Hanbook of Ferromagnetic Materials, Amsterdam, North-Holland, vol. 3, 1982, 441–602.
[26] R.A. McCurrie, G.P. Carswell, Magnetic hardness of the intermetallic compound $SmCo_5$as a function of particle size, Phil. Mag. 23 (1971) 333–343.
[27] P. Nothnagel, K.H. Muller, D. Eckert, A. Handstein, The influence of particle-size on the coercivity of sintered NdFeB magnets, J. Magn. Magn. Mater 101 (1991) 379–381.
[28] R. Ramesh, K. Srikrishna, Magnetization reversal in nucleation controlled magnets .1. Theory, J. Appl. Phys. 64 (1988) 6406–6415.
[29] H. Sepehri-Amin, T. Ohkubo, M. Gruber, T. Schrefl, K. Hono, Micromagnetic simulations on the grain size dependence of coercivity in anisotropic Nd-Fe-B sintered magnets, Scr. Mater 89 (2014) 29–32.
[30] K. Uestuener, M. Katter, W. Rodewald, Dependence of the mean grain size and coercivity of sintered Nd-Fe-B magnets on the initial powder particle size, IEEE Trans. Magn. 42 (2006) 2897–2899.